Chemical Physics Letters 481 (2009) 153–165

Contents lists available at ScienceDirect

Chemical Physics Letters

journal homepage: www.elsevier.com/locate/cplett

FRONTIERS ARTICLE

Optical control and characterisation of aerosol

Jon B. Wills, Kerry J. Knox, Jonathan P. Reid *

School of Chemistry, University of Bristol, Bristol BS8 1TS, UK

ARTICLE INFO

Article history:
Received 14 August 2009
In final form 6 September 2009
Available online 10 September 2009

ABSTRACT

Aerosols are ubiquitous throughout the environment and find numerous technological applications yet a comprehensive understanding of their properties and processes remains elusive. Optical tweezing has emerged as a technology that opens a microscopic window through which we can study aerosols in exquisite detail. In this publication, we describe state of the art measurements of hygroscopicity, phase, supersaturation and mass accommodation. Further, we discuss how the precision and elegance of aerosol tweezer measurements can provide a platform for micro-scale chemical and biological assays as well as a unique perspective on more general problems in physical chemistry and chemical physics.

1. Introduction

Aerosol particles play an important role in a broad range of scientific disciplines, extending from their use in the pharmaceutical industry, to their impact on air quality and human health, their technological application in spray drying, the delivery of fuels for combustion, and their impact on regional and global climate. Despite the importance of aerosols, characterising their properties and probing their transformation remain challenging. Properties are frequently inferred from the study of macroscopic phases, ignoring the importance of the surface-to-volume ratio. Sampling artefacts often compromise the analysis of aerosol samples. Measurements of particle size distributions are often seen as a panacea for interpreting aerosol properties and the significance of chemical composition is often neglected. The experimental challenges of directly studying evolutions in particle size, composition and temperature can often be too insurmountable to fully characterise the mass and heat transfer that occur during particle evaporation or growth.

Addressing the fundamental chemical and physical concepts that underpin the properties of aerosols and the processes that are responsible for their transformation is demanding and habitually frustrated by intractable analytical challenges. In many instances the complexity of an aerosol, arising from the heterogeneity in particle size, composition, phase, and mixing state, is further complicated by the inherently rapid coupling with the surrounding gas phase. Indeed, a gulf exists between the benchmark simplified systems that are routinely studied in controlled laboratory measurements and the highly variable and complex aerosols observed in, for example, the atmosphere.

Despite the ever-persistent need to address the challenge of complexity, it is imperative to recognise that a fundamental chemical and physical foundation is always required if observational trends are to lead to robust predictive capability. In reality, many of the problems that must be addressed to more completely understand aerosols are a reflection of more fundamental questions that must be answered to understand the dynamics and heterogeneity of liquid and solid surfaces, the kinetics and pathways of condensed phase reactions, the thermodynamics of multicomponent solutions and phases, the optical properties of materials, and the kinetics of nucleation.

Laboratory techniques for investigating aerosol properties and processes focus on studying single particles, particle ensembles, or on deriving aerosol properties from studies of bulk phases or flat surfaces. Measurements on particle ensembles, usually selected narrow size ranges of accumulation mode particles (1 μm diameter), are able to provide a rapid assessment of a statistically averaged property, allowing the robust investigation of aerosol optical properties [1–3], hygroscopicity [4], chemical aging [5–8] and phase behaviour [9–11]. Studies of bulk phases or flat surfaces, once corrected for the change in length scale, have provided important information on chemical processes [12–14], optical properties [15], solution thermodynamics and hygroscopicity [16].

Single particle studies, while requiring care in extrapolating to the ensemble level, can bridge the gap between aerosol ensembles and bulk/surface properties. Studies have yielded important insights into chemical reactivity [17–19], equilibrium particle size, composition and hygroscopicity [20–25], optical scattering and absorption [26,27], and the kinetics of mass and heat transfer [28,29]. In addition, single particle studies could provide an ideal opportunity to address the challenges of complexity, allowing a hierarchical progression from simple benchmark single component systems to a mixed phase/multicomponent condensed phase while retaining the ability to explore aerosol processes at a fundamental

* Corresponding author. Fax: +44 0117 925 0612.
E-mail address: j.p.reid@bristol.ac.uk (J.P. Reid).

0009-2614/$ - see front matter © 2009 Elsevier B.V. All rights reserved.
doi:10.1016/j.cplett.2009.09.020

level. Indeed, in somewhat of a role reversal, as we will show in this article, single aerosol particle studies could be used as an ideal tool for addressing a number of fundamental questions in physical chemistry/chemical physics.

Approaches for sampling and characterising single aerosol particles have included instruments that isolate single particles in electrostatic, acoustic and optical traps [30–32]. In this Letter, we will concentrate on the use of optical traps, focussing specifically on recent developments in forming tailored optical traps rather than more conventional particle levitation that is achieved through the action of radiation pressure. Once recent developments in optical manipulation have been reviewed, we will consider the armoury of techniques that can be used to interrogate trapped particles and the control that must be exerted over environmental conditions. Finally, we will consider the scientific frontiers that can be explored through studies of single particles or through parallel measurements on multiple particles.

2. The manipulation of aerosol particles with light

Born from the classic works of Maxwell is the remarkable idea that light can be used to manipulate matter through the action of light pressure, also referred to as radiation pressure. At the turn of the 20th century, Lebedev was the first to demonstrate through laboratory measurements that electromagnetic radiation exerts a pressure [33]. However, it was almost seven decades before Ashkin reported the first practical application following the development of the laser [34]. The optical forces exerted on microscopic objects by a focussed laser beam are commonly in the range 10 fN to 100 pN, providing an ideal tool for probing and manipulating the nano- and micro-worlds [35,36]. In this Letter, we focus our attention on the manipulation of aerosol particles, although it is important to recognise at the outset that considerable research has centred on controlling particles in the condensed phase.

2.1. Optical levitation and optical tweezing

In his first demonstration of the effects of radiation pressure on microscopic particles, Ashkin reported that micron-sized polystyrene particles suspended in water and water droplets in air were accelerated along the direction of laser beam propagation [34]. Ashkin went onto show that solid particles and liquid droplets, could be stably supported in air using a vertically propagating weakly focussed laser beam, with the downward gravitational force balanced by the upward scattering force, or radiation pressure [37,38]. Ashkin demonstrated that two particles could be levitated and translated independently by using multiple beams [39]. In addition to the supportive effect of radiation pressure, it was noted that a second weaker force acted to restore the particle to the central, most intense, region of the light beam [34,40].

The interaction of light and dielectric materials has been the subject of much debate for over 100 years [41]. Indeed it is not clear as to whether light exerts a push or pull on dielectric media. The discussion has become known as the Abraham–Minkowskii controversy after the two physicists responsible for the contradicting theories [42,43]. Qualitatively, the interaction of a focussed laser beam with a microparticle is often described by two parts, a scattering component and a component dependent on the gradient of the electric field associated with the optical beam. The scattering force is rationalised in terms of a transfer of momentum to the dielectric particle from backscattered photons. If the illumination is a pure plane-wave, then this is the only optical force that need be considered and, intuitively, it acts to push the particle along the beam propagation direction. In a levitation trap, the beam is gently focused and a particle adopts a stable position within the divergent beam above the focus. At this unique equilibrium position, the downward gravitational force is exactly balanced by the upward scattering force.

Once a spatially varying illuminating beam intensity is considered, such as that achieved with a gently focussed beam which has a Gaussian intensity profile transverse to the propagation direction, micron-sized dielectric particles are observed to migrate towards the region of high light intensity due to the action of the gradient force [34,40]. For spherical particles, it is possible to qualitatively demonstrate this effect by considering a ray optic model. In Fig. 1a, two parallel rays are shown passing through a spherical particle, the central axis of which lies equidistant between the rays. Depending on the refractive indices of the two media, the rays are refracted equally and in opposite directions and a transfer of momentum between the light and the particle can be envisaged to occur at the point of refraction. If the rays are equal in intensity, as is the case for a particle levitated symmetrically at the centre of a Gaussian beam, the gradient forces from the rays will be equal and opposite. If, however, the particle is displaced from the central axis of the beam, then one ray will have greater intensity than the other. Thus, the resultant gradient force will draw the particle towards the more intense ray and the central axis of the beam.

Levitation traps are intrinsically delicate and unstable. While the axial component of the optical force is equal to the weight of the particle at all times, the gradient force acting transverse to the beam propagation direction is weak and air currents can be enough to destabilise the trapped particle. An increase in laser power, although initially increasing the gradient component, increases the scattering force and thereby displaces the particle further from the beam focus to a new equilibrium position where the beam has diverged, which has the affect of reducing the lateral stiffness of the trap. Aligning two, weakly focussed counter-propagating beams overcomes this problem and can create a very stable trap for particles in liquid [34] or in gas [44,45]. Alternatively, it has recently

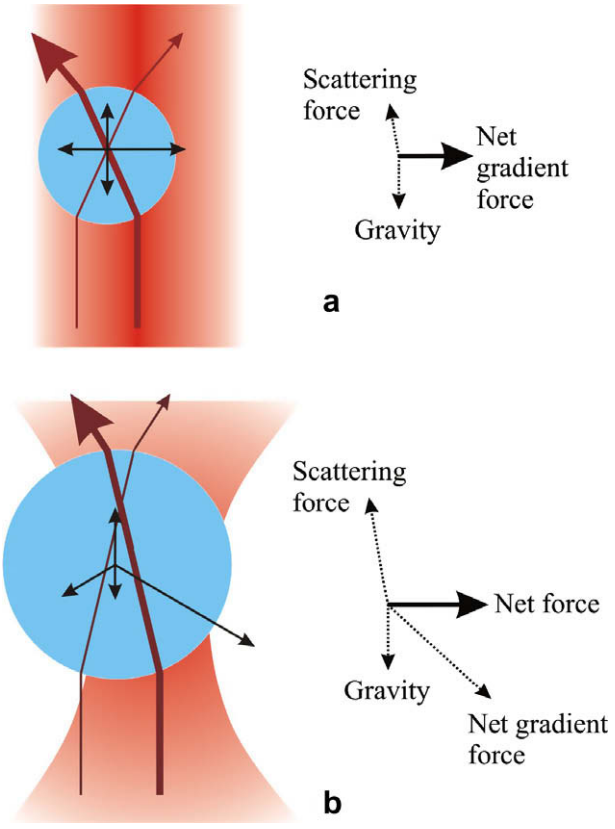

Fig. 1. Schematic representation of optical trapping forces in a Gaussian beam (a) and a gradient force optical tweezer (b).

been shown that divergent beams from opposing optical fibres in close proximity can be used in place of a conventional beam manipulated by lenses and mirrors, forming what is commonly referred to as a fibre-trap [46].

The contribution of the gradient force can be grossly amplified by using a microscope objective lens to tightly focus the trapping laser beam forming a single beam gradient force optical trap, or optical tweezers [47]. This effectively creates a strong intensity gradient in three dimensions, leading to strong transverse and axial restoring forces that are many orders of magnitude larger than the gravitational force acting on the particle. Thus, particles can be captured and held tightly against the scattering and gravitational forces. Omori et al. showed that it was possible to optically tweeze dielectric particles in air [48], while Magome et al. were the first to demonstrate the optical tweezing of liquid particles in air [49]. Again, a simple ray optics analysis can be used to explain the forces acting on the particle (Fig. 1b). The position of the trap can be adjusted by varying the angle of incidence of the trapping laser with the back aperture of the objective lens.

It follows that by passing multiple beams through the same objective lens at different angles of incidence we can begin to build up simple optical landscapes with multiple traps that can be used to simultaneously manipulate several particles, as illustrated in Fig. 2. Using a beam splitter and two mirrors, both conjugate with the back aperture of the objective, it is relatively straightforward to generate two independently translatable traps [50]. This technique has been applied extensively to the tweezing of aerosol droplets. Comparative measurements of thermodynamic and kinetic properties are possible, as well as studies of controlled droplet coalescence and mixing dynamics [51–54].

2.2. Higher-order optical beams and optical landscapes

So far we have only considered zeroth order beams with a cross-section that has a Gaussian intensity profile. Although lasers are typically optimised to output zeroth order beams, through deliberate misalignment of the laser cavity or with additional optical components, it is possible to generate higher-order-mode beam shapes that have useful attributes for optical manipulation. Indeed, both Hermite–Gaussian (HG) [55] and Laguerre–Gaussian (LG) [56] laser beams of mode order higher than zero can be used to manipulate the orientation of trapped particles in liquids and, more recently, in air (Fig. 3) [57]. In the first case, the trapped particle can be rotated by rotating the beam, applying a torque to the material. In the latter case, spin and/or orbital angular momentum is transferred to the particle through the intrinsic 'corkscrew' phase pattern of LG beams.

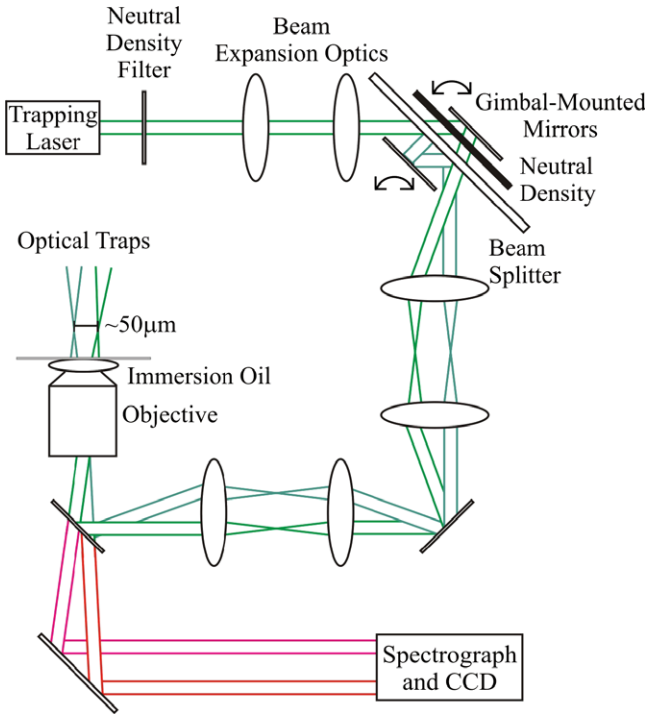

Fig. 2. Schematic illustration of the dual trapping configuration for trapping and manipulating two aerosol particles. Reproduced with permission from Ref. [103].

One limiting factor of aerosol optical tweezing is the length scale over which manipulation can be performed, which is restricted to about ~100 μm transverse to the beam propagation direction through beam steering and trap translation, and a few tens of micrometres axially through translation of the beam focus. A tight optical focus, although enabling robust particle confinement, restricts the particle to the focal region and precludes the routine capture of multiple particles within one trap.

To a significant extent, the limitation of operational length scale can be overcome by employing a Bessel beam. Such beams have a transverse profile that is composed of a bright core and a series of concentric rings, as illustrated in Fig. 4. Theoretically, the rings are infinite in number and equal in integrated intensity/photon flux to that of the core. A true Bessel beam would not suffer from diffraction and although such a beam cannot be realised in the laboratory, it is possible to generate a pseudo non-diffracting Bessel beam over a finite propagation distance using a conically-shaped lens, referred to as an axicon [58]. The Bessel beam can be considered to arise from the interference resulting from rays propagating on the surface of a cone, with constructive interferences occurring along the central beam axis. It is possible to generate such beams with core widths of just a few microns, approaching the focal waist of optical tweezers, yet without the axial constraint. Bessel beams have been applied to translating aerosol droplets over distances of up to 2.5 mm along the beam propagation direction by controlling the beam power [57]. The core of such beams is near non-diffracting, typically with a diameter of <10 μm extending over millimetres. In comparison with Gaussian beams, the intrinsic divergence of a collimated Gaussian beams is defined by the Rayleigh range, Z_r, which defines the distance over which the beam cross-section doubles and which is a function of the beam waist, w_o:

$$Z_r = \frac{\pi w_o^2}{\lambda},$$

where λ is the wavelength of the light forming the beam. The Rayleigh range of a 532 nm Gaussian beam with waist 5 μm is just 0.15 mm.

Furthermore, a Bessel beam exhibits the invaluable property of self healing: a beam will reconstruct after a characteristic length scale if it encounters an obstruction such as a trapped particle. Thus, multiple particles can be isolated within a single beam and their position controlled by controlling the laser power. An additional, unsolicited, advantage of the Bessel beam trap is the ability to manipulate sub-micron diameter particles, representative of the aerosol accumulation mode [59].

Using passive optical elements to design a system with more than two independent traps becomes increasingly complex and impractical. Further, reconfiguration of an optical tweezer apparatus to adjust the number of traps or the beam mode order requires a significant investment of time. These limitations can be greatly diminished by using active, computer-controlled optical components [60,61]. These devices commonly employ a spatial light modulator (SLM) to manipulate the phase and intensity profile of an incident Gaussian laser beam. For example, higher order beams

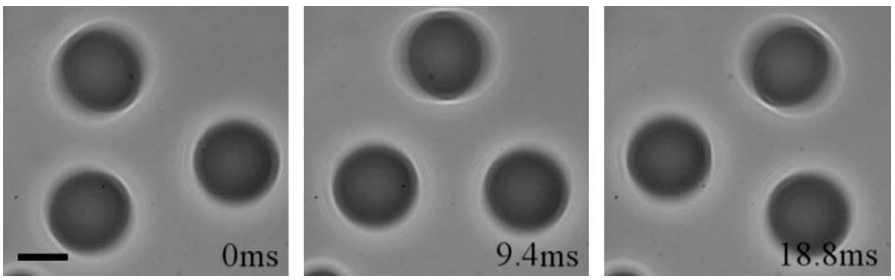

Fig. 3. Three aqueous aerosol droplets trapped within a Laguerre–Gaussian beam imaged as a function of time. Transfer of orbital angular momentum is clearly evident in the three images as the array undergoes rotation. Ref. [57] –Reproduced by permission of The Royal Society of Chemistry.

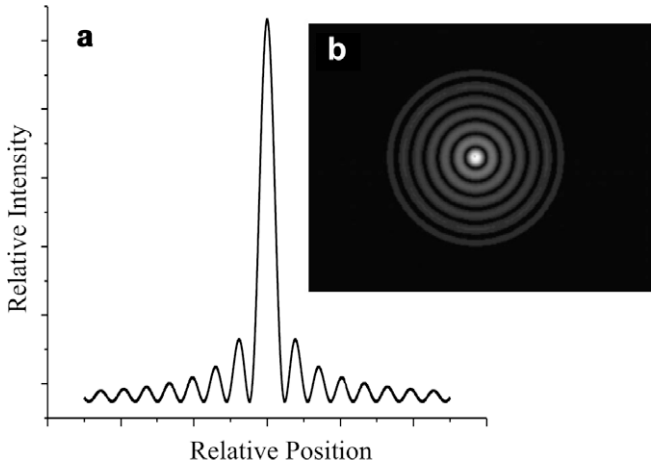

Fig. 4. (a) Two dimensional, zeroth order squared Bessel function. (b) Transverse profile of an optical Bessel beam.

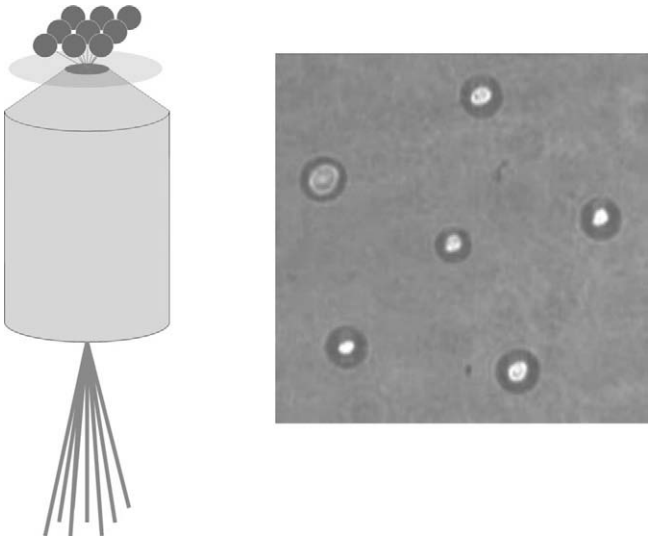

Fig. 5. An optically-tweezed array of aerosol droplets: schematic representation of a nine trap array (left), and brightfield image of a carousel array of trapped droplets (right).

can be created, as can multiple, parallel Gaussian beams, each of which can be used to trap a particle. The SLM can typically be updated at around 100 Hz, and is controlled *via* a computer interface. This creative ability can generate an evolving optical landscape that can be designed to change quickly and dramatically or slowly and sequentially over time. After the holographic phase patterns that are displayed on the SLM, optical tweezers that incorporate such devices have become known as holographic optical tweezers (HOTs) [61,62].

In a similar way to the dual trap discussed earlier, HOTs have been used to simultaneously tweeze arrays of aerosol droplets [62]. Reid and co-workers used a carousel array arrangement to facilitate the sequential interrogation of each droplet through global rotation of the array [63]. In this way comparative measurements of aerosol properties have been performed and controlled sequential coalescence demonstrated. Fig. 5 shows a schematic representation of a tweezed aerosol array and a brightfield image of a carousel array containing five droplets around a centrally trapped sixth droplet.

One of the most interesting applications of HOTs is the potential to generate arbitrary optical landscapes. These may consist of any number (within reasonable limits set by the available laser power and the resolution and damage threshold of the SLM) of traps of varying type along with other regions of light intensity. Working in the two-dimensional focal/trapping plane of the tweezer microscope objective, optical barriers can be designed to direct free-flowing aerosol in addition to forming traps to catch particles [64]. This approach has facilitated comparative studies of dissimilar aerosol droplets simultaneously and in the same gas phase, as well as the use of a single droplet as a highly sensitive probe of gas-phase composition within aerosol media.

Fig. 6 illustrates a simple application of a tailored optical landscape to isolate a trapped aerosol droplet from free-flowing droplets in the trapping cell. In parts (a) and (b) aerosol is flowing through the cell from bottom left to top right, the solid shaded circle in the centre of the plot is representative of a trapped droplet and the lines shown illustrate the trajectories of free flowing droplets. The points on the trajectories show the free flowing droplet position for sequential video frames and thus the velocity and acceleration of these free flowing droplets can be determined [64]. In (a) free droplets are seen to pass unperturbed through the trapping cell; however, those that pass close to the trapped droplet are drawn in and may coalesce with it. In (b) an intense ring of light around the trapped droplet, illustrated by the dashed circle, is applied to scatter free droplets away from the central trap. Droplets are seen to be accelerated around or, more commonly, over the isolated trapping region. Fig. 6c shows the recorded size of the trapped droplet as a function of time whilst aerosol is flowed through during the two experiments. The efficacy of the circular optical shield in isolating the trapped droplet is clear to see. This technique has been used to load two dissimilar droplets into neighbouring traps for comparative studies and also to isolate an aerosol probe droplet from interactions with the aerosol medium under investigation.

3. Particle characterisation

A number of strategies can be applied to characterise optically-trapped aerosol droplets, including the observation of

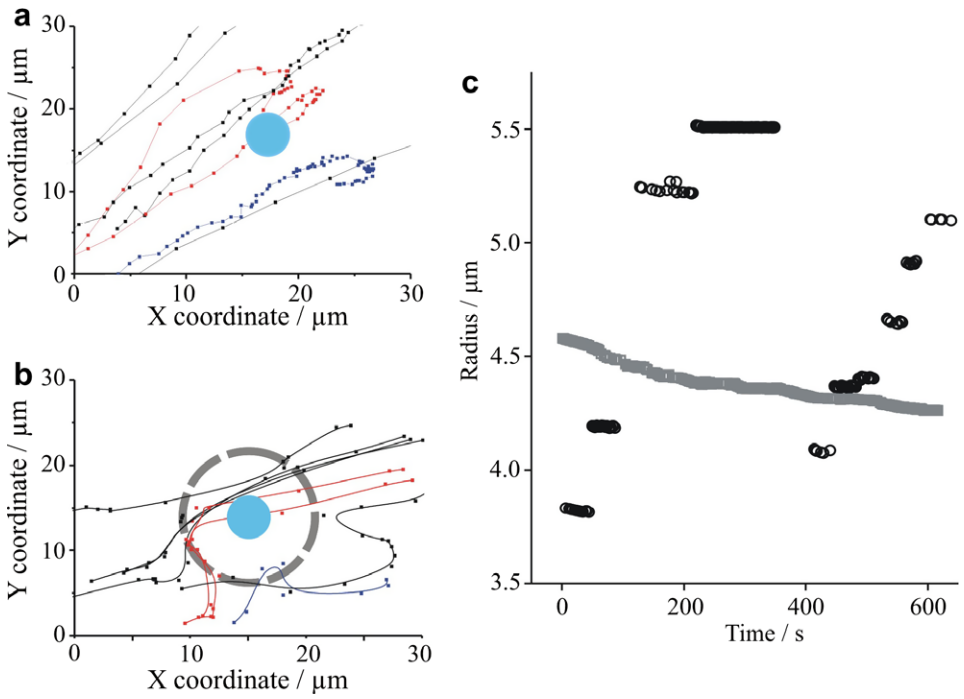

Fig. 6. Demonstration of droplet isolation by holographic optical trapping. (a) Trajectories are shown for aerosol droplets flowing freely through the trapping cell and passing a centrally trapped droplet – two of the free droplets are observed to coalesce with the trapped droplet. (b) As in (a), however, a circular optical barrier is applied (shown schematically by the dashed circle), inhibiting coalescence with the trapped droplet. (c) The time dependence of the droplet sizes clearly demonstrates the successful isolation of the trapped droplet by the circular optical barrier (size for case shown in (a) – black circles, and for (b) – grey squares). Ref. [64] – Reproduced by permission of the PCCP Owner Societies.

elastically-scattered light, the measurement of a Raman or fluorescence fingerprint, and the application of conventional brightfield microscopy. While the characterisation of particle size will feature strongly in this section, size represents only one of a wide range of properties of optically-trapped particles which can be investigated and we will also consider the characterisation of composition, refractive index and mixing state [65].

3.1. Brightfield imaging

Brightfield imaging techniques can be used to provide a measure of droplet size, to probe droplet structure and to investigate the optical forces experienced by a tweezed aerosol droplet. Two-dimensional images can be recorded of the horizontal trapping plane, or of the vertical plane using a zoom lens and camera mounted to record a side image. In the case of imaging in the plane of the optical trap, the droplets are typically illuminated with light from an LED and the trapping microscope objective is used to collect the imaging light, which is directed towards a CCD camera. Typical in-plane and side images are shown in Fig. 7.

While in-plane imaging can be used to determine droplet size, several factors limit the accuracy to ±0.2 μm [66]. Because the trapping objective is not optimised for imaging in air and because of the high refractive index mismatch between the droplet and the surrounding medium, the image resolution is poor and hence locating the droplet boundary is difficult [66]. Further, it has been demonstrated that the aerosol droplet trapping position, and hence position relative to the collection optics, exhibits considerable variation with particle size, laser power and trapping conditions, behaviour which is not observed in condensed phase optical tweezers [67]. As a result, image-based methods for determining the size of tweezed aerosol particles offer limited accuracy and a spectroscopic method should ideally be employed.

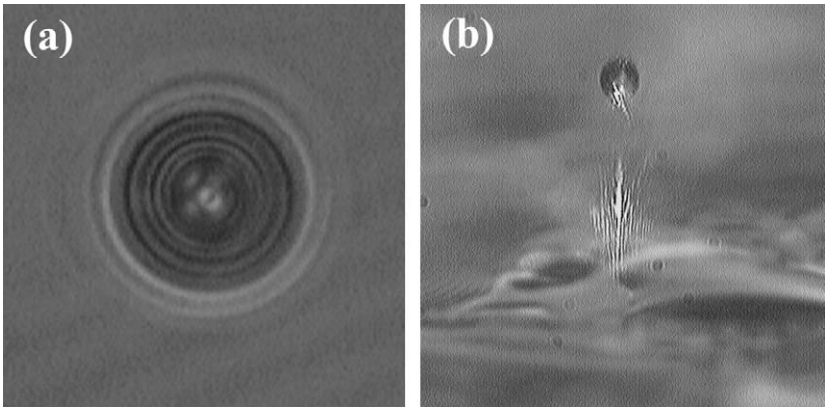

Fig. 7. Brightfield microscopy images of optically-tweezed droplets recorded (a) in-plane and (b) from the side.

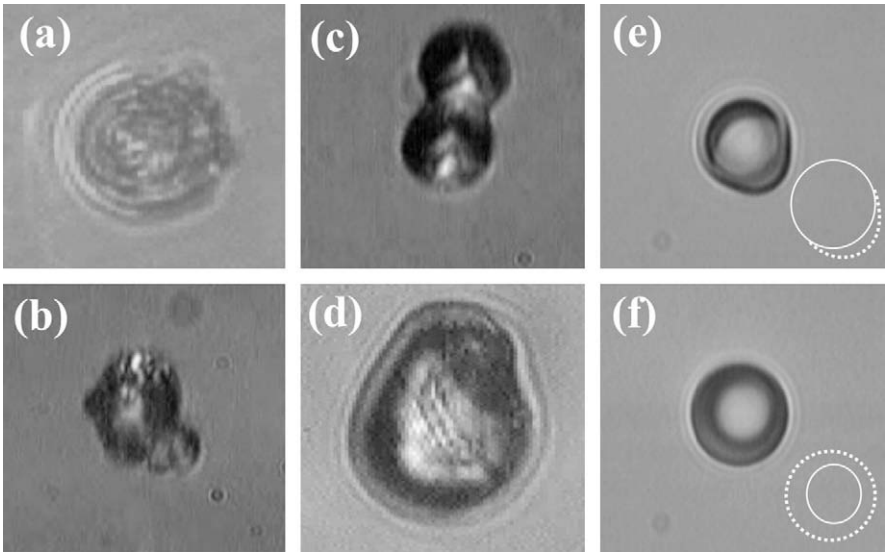

Fig. 8. Examples of the microphysical structures of particles formed in the optical trap: (a) a hydrated insoluble palmitic acid crystal within a host aqueous droplet; (b–d) microgel particles of surfactant; (e–f) multiphase droplets containing hydrophobic (decane) and hydrophilic phases (aqueous sodium chloride).

Imaging techniques can be used to identify the phase of a particle and to investigate the evolving micro-structure of a mixed-phase particle (Fig. 8). The formation of insoluble inclusions within droplets has been observed in the case of an aqueous sodium chloride droplet containing the insoluble surfactant palmitic acid [68]. The palmitic acid inclusions were observed to occur both within the bulk and at the edge of the droplet. Phase transitions occurring in aqueous sodium chloride droplets containing the surfactant sodium dodecyl sulfate (SDS) have also been monitored, including the transition from a liquid droplet to a metastable microgel particle and the adhesion of two solid SDS/sodium chloride microgel particles following coagulation [69]. The phase segregation of immiscible decane and aqueous components within a single liquid aerosol droplet has been observed using brightfield microscopy [70]. These multiphase droplets were formed by bombarding optically-trapped aqueous droplets with a nebulised flow of decane. The equilibrium microphysical structures formed were found to be consistent with those predicted by the approach of Torza and Mason, which considers the volume fraction of each immiscible component and the interfacial tensions involved [71,72].

Side images, recorded at 90° to the direction of trapping beam propagation, have been used to gain insights into the forces operating in aerosol optical tweezers. In particular, the vertical displacement of optically-tweezed droplets along the direction of the laser propagation, referred to as the axial displacement, has been studied directly [67]. Indeed, the sensitivity of the axial displacement to changes in the trapping laser power was shown to provide a coarse measure of droplet size.

In addition to observing trapped particles, free-flowing aerosols within the trapping cell can also be monitored using bright field microscopy. In this way, Reid and co-workers have been able to record droplet trajectories and determine forces acting on free droplets passing through a trapping cell and interacting with the optical landscape [64].

3.2. Spontaneous Raman spectroscopy

Raman fingerprints recorded from trapped aerosol droplets can be used to provide information on droplet size, structure and composition [73]. Referred to as cavity-enhanced Raman spectroscopy (CERS), spectra comprising of both spontaneous and stimulated Raman scattering are commonly collected [73]. A typical CERS spectrum from an aqueous sodium chloride droplet is shown in Fig. 9. The light recorded arises from excitation of the O-H stretching vibrational modes of water, occurring at a Stokes shift between ~3100 and ~3700 cm^{-1}. The underlying, spontaneous Raman band shape is punctuated by sharp features which correspond to stimulated Raman scattering, the threshold for which is surpassed at wavelengths commensurate with cavity resonances of the droplet, commonly referred to as whispering gallery modes (WGMs) or morphology dependent resonances. In the case of optically-tweezed aerosol droplets, the 532 nm trapping laser beam is used as the excitation source for the Raman scattering, and as the tweezed droplets are held with high positional stability close to the tight laser focus created by the microscope objective, this objective is also used to collect the Raman-scattered light with high efficiency. Thus spectra are collected with high signal-to-noise ratios, even for small droplets (<2 μm in radius) and short spectral acquisition times of <1 s.

Spontaneous Raman scattering can be used to probe droplet composition, with Raman-active molecular species giving rise to

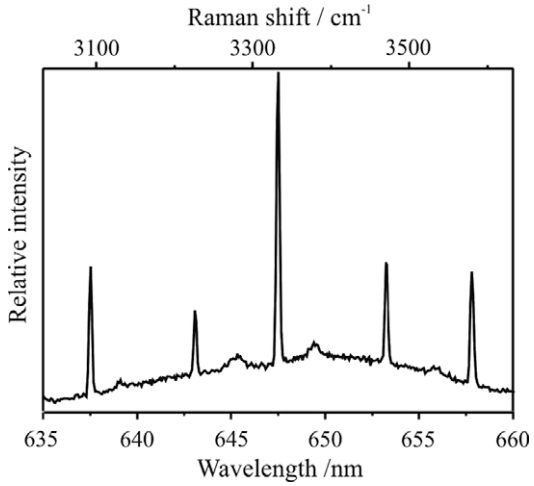

Fig. 9. A typical Raman spectrum (532 nm illumination) collected from an aqueous sodium chloride optically-tweezed droplet showing the broad spontaneous band arising from the O–H stretching vibrational modes of water with cavity-enhanced resonance structure superimposed arising from stimulated Raman scattering.

characteristic Raman shifts and signals. For example, the presence of a signal at a shift of ~2850 to ~2950 cm^{-1}, characteristic of C–H stretching vibrations, demonstrates that the droplet contains an organic species. This spectral signature has been used to investigate the evolving composition during the evaporation or condensation of gaseous organic components from or to an aqueous droplet and the deposition by coalescence of small organic aerosol particles [69,74]. Further, the shape of the Raman O–H band provides a measure of the distribution of hydrogen bonding environments within an aqueous droplet, and can be used as a measure of the ionic strength of droplets containing inorganic solutes and to confirm the phase separation of hydrophobic and hydrophilic phases in a mixed phase droplet [74]. The detection limit of typical Raman scatterers, such as nitrate and sulphate with Raman cross-sections of 1×10^{-28} cm^2 $molecule^{-1}$ sr^{-1}, can be shown to be ~10 mM with the detection limit set by the shot-noise limit of the typical CCD detectors used to record the dispersed Raman fingerprint [75].

As it provides a signature of droplet composition, spontaneous Raman spectroscopy can be used to follow the progress of aerosol phase chemical reactions. King et al. have used the evolving intensity of characteristic Raman signals to follow the decay of reactants and evolution of chemical products during the oxidation by gas-phase ozone of an optically-tweezed oleic acid/water droplet [76] and of tweezed aqueous or organic droplets containing fumarate anions, benzoate anions or α-pinene [77].

3.3. Stimulated Raman spectroscopy

The wavelengths of the WGMs are dependent on the size of the optical cavity (which is dependent on the radius of the droplet) and can be predicted using Mie scattering theory. Thus, by comparing the wavelengths of resonances appearing in a microdroplet Raman spectrum with theoretical predictions from Mie theory the droplet size can be determined. Provided that the refractive index of the droplet is accounted for, the size of micrometre radius droplets can be determined with nanometre accuracy [73,78].

The WGMs can be assigned a mode number, *n*, polarisation, *P*, and mode order, *l* [79]. The mode number defines the number of wavelengths forming the standing wave in the electromagnetic field circulating the droplet circumference. Modes with no radial dependence in the electric component of the field are defined as modes of transverse electric (TE) polarisation and modes with no radial dependence in the magnetic component as transverse magnetic (TM). The mode order specifies the number of maxima existing in the radial dependence of the mode intensity.

By using CERS to determine the evolving droplet size of optically-tweezed aerosol with high precision, a wide range of aerosol properties and processes have been investigated, including the thermodynamic properties of aerosol, the kinetics of size equilibration and the presence of an organic film on the surface of an aqueous droplet [73]. Determining the variation of the equilibrium size of mixed composition aerosol particles with the surrounding relative humidity (RH) is not straightforward and the quantitative understanding of this for multi-component organic/inorganic/aqueous atmospheric aerosol particles remains limited [80]. Reid and co-workers have recently demonstrated a technique for investigating the thermodynamic size of complex mixed-component aerosol which provides an unprecedented level of accuracy in recording the equilibrium size variation of a droplet with variation in RH [52,53]. The technique involves establishing a pair of optical traps which can be used to isolate two droplets simultaneously. In one trap, a droplet containing a mixture of organic and inorganic solutes, representative of atmospheric aerosol, is captured. In the second trap, a 'control' droplet containing a single inorganic salt, usually sodium chloride, is isolated and used as a highly accurate and responsive microscopic probe of the local RH, with an accuracy of better than ±0.09%. Through measurement of the subsequent evolution in size of both droplets, the hygroscopic behaviour of the mixed component droplet of interest can be rigorously characterised and compared with theoretical predictions.

The ability to specify subsets of CCD pixels on the detector used to record the wavelength dispersed CERS fingerprint allows the signals from more than one droplet to be collected simultaneously. By directing the light from each of two simultaneously-trapped droplets to different vertical regions of the CCD detector, signals can be recorded separately and simultaneously. This procedure is shown schematically in Fig. 2 for a dual optical tweezers configuration. Fig. 10a shows an image of the scattered light from two simultaneously-trapped droplets falling on the CCD. The resulting droplet spectra are shown (part b), each integrated over seven horizontal rows of CCD pixels, along with a brightfield image of the two trapped droplets (part c). Spectra can then be acquired from each droplet with a time resolution of 100 ms.

As well as providing a highly precise measure of droplet size, CERS can also be used to characterise the structure of mixed composition droplets. Particles with a core–shell structure give rise to distinctive CERS spectra for which adjacent cavity resonances of opposing polarisation are not spaced in wavelength by the amount expected for a homogenous droplet. By comparing these spectra with predictions from Mie calculations of scattering from layered core–shell spheres, the radius of the core and the thickness of the shell can be determined. Buajarern et al. have used this approach to probe the evolving phase partitioning in multiphase decane/aqueous sodium chloride droplets [81].

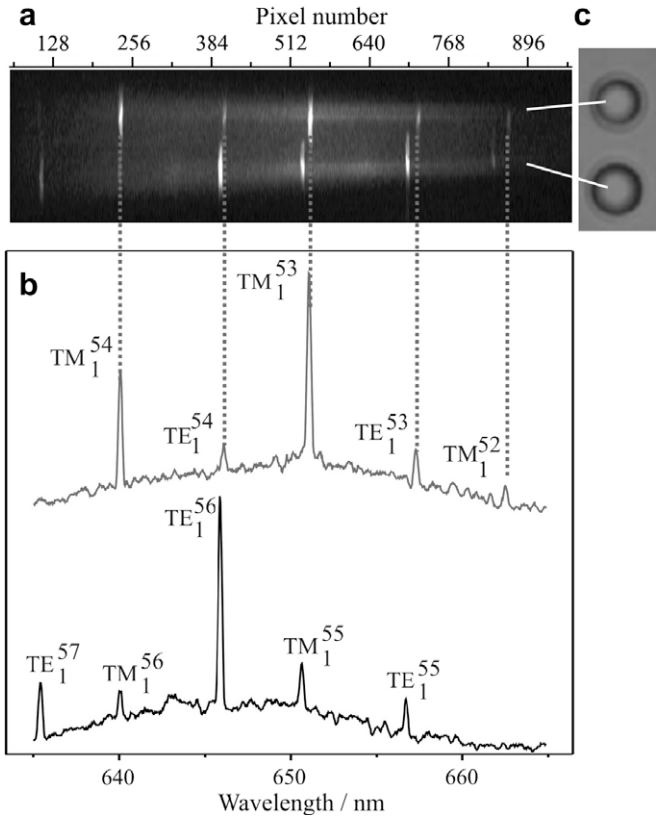

Fig. 10. Simultaneous measurement of the Raman fingerprints of two trapped droplets. (a) The image of the dispersed inelastically-scattered light from the two droplets falling on the CCD. (b) The spectra from the two droplets with mode assignment. (c) A brightfield image of the droplets illustrates that the droplets are aligned to the vertical axis of the entrance slit to the spectrograph and hence to the vertical axis of the CCD detector.

As a result of the non-uniform illumination of the droplet in optical tweezers, Raman spectroscopy can provide an insight into the microphysical structure of a trapped droplet, including the motion of an inclusion within a host droplet. The position of a sub-micron polystyrene bead within an aqueous droplet can be diagnosed by the presence or otherwise of hydrocarbon Raman shifts and resonant structure in the CERS. The intensity of the former depends on the varying extent of illumination of the inclusion in different regions of the droplet. The absence of the latter indicates that the inclusion resides in the cavity mode region near the surface of the droplet [68]. This approach has been used to confirm that an insoluble palmitic acid inclusion within an aqueous droplet can reside either at the surface of the droplet or be found diffusing within the droplet bulk, consistent with in-plane brightfield images of the mixed phase droplets [68]. By examining the autocorrelation of the CH and OH Raman intensities arising from the inclusion and host, respectively, the timescale for diffusion of the inclusion throughout the entire host volume was probed.

A limitation associated with using CERS for the determination of droplet size is that it is difficult to apply to droplets with a radius of <2 μm. This is a result of the spacing between cavity modes increasing with decreasing particle size, leading to a decreasing number of cavity modes which fall within with the bandwidth of a given Raman signal [73,79]. Further, the quality factor of the cavity modes diminishes with decreasing droplet size, resulting in broad, poorly-defined resonances [82]. Several methods of sizing appropriate for particles of <2 μm in radius are discussed in the following two sections.

3.4. Elastic light scattering

The interference and ripple structure characteristic of the variation in light scattering intensity with particle size parameter in the Mie regime can provide a versatile tool for characterising the size of droplets of all sizes. Ward et al. have demonstrated the use of a broadband white LED as an illumination source for elastic scattering by aqueous sodium chloride droplets [83]. Mie resonances were observed over the spectral range 480–700 nm, allowing the sizing of droplets of 2–8 μm in radius with a precision of ±2 nm. Further, Guillon and Stout used linearly polarised light from an LED with a bandwidth of 50 nm to determine the size of trapped oil droplets with radii as low as 1.29 μm.

An alternative approach is to measure the phase function of elastically-scattered light to determine the size of the scatterer. Here, the scattered light is collected using a simple CCD camera, examining the angular variation in the intensity of the scattered light. This approach has been used to determine the diameter of aqueous droplets as small as 1.7 μm, isolated using a Bessel beam [59]. By using the phase function method to calibrate the brightfield microscopy image obtained using a zoom lens system, it was confirmed that a Bessel beam could be used to manipulate particles smaller than 1 μm, the first direct evidence that optical techniques can be used to manipulate and characterise accumulation mode aerosol.

3.5. Fluorescence spectroscopy

The addition of fluorescent chromophores to optically-isolated droplets offers further possibilities for droplet characterisation. By incorporating a dye with a pH dependent fluorescence spectrum into an optically-isolated droplet, the droplet composition can be investigated. Preliminary measurements on aqueous optically-tweezed aerosol droplets containing acridine have indicated that the kinetics of uptake of the atmospherically-relevant soluble base ammonia from the gas phase should be possible [84]. Further, the addition of a fluorescent chromophore to a microdroplet can offer a further solution to the problem associated with the restricted bandwidth of typical Raman signals. Fluorescence emission profiles commonly span several hundred nanometres. Therefore, the resonant structure of the fluorescence spectrum can be used to size smaller droplets than is possible with CERS. This is useful for sizing small droplets provided that the addition of an absorbing chromophore at concentrations of $\sim 10^{-6}$ M does not significantly influence the aerosol property it is sought to investigate.

An example of a cavity-enhanced fluorescence spectrum is provided in Fig. 11 for an aqueous sodium chloride droplet which has been bombarded with aqueous aerosol containing Rhodamine B at a concentration of 8.7×10^{-6} M. Once the dye is incorporated within the trapped droplet, the cavity resonance structure can be seen to extend beyond the Raman O–H band region, commensurate with the fluorescence emission band of Rhodamine B. The broken line shows the normalised fluorescence emission intensity of Rhodamine B. It can be seen that the intensity profile of the cavity-enhanced fluorescence spectrum follows the intensity trend of the bulk fluorescence spectrum for modes of the same polarisation and order, consistent with that observed in Raman scattering fingerprints. This is an example of using a controlled dosing in the aerosol phase to analyse aerosol.

3.6. Light absorption measurements on trapped aerosol

Reid and co-workers have recently reported a technique for determining the absorption coefficient of optically-tweezed aerosol droplets [85]. The vapour pressure of water at the surface of an aqueous droplet is determined by the droplet temperature and the solute concentration for droplets with radii >1 μm, typical in our work. Although the complex part of the refractive index of water is very low ($<1 \times 10^{-8}$) at the trapping wavelength (532 nm), a trapped droplet can be shown to be elevated in temperature above the surroundings by a few tens of milli-Kelvin.

If a change in the incident irradiance is instigated through a change in the trapping laser power, a droplet temperature change is induced. This results in a response in droplet size which can be monitored by CERS. The droplet must adjust in size to achieve a new solute concentration at which its vapour pressure, at the modified temperature, once again balances the surrounding RH. The effect can be seen clearly in Fig. 12; the shift of the resonant modes

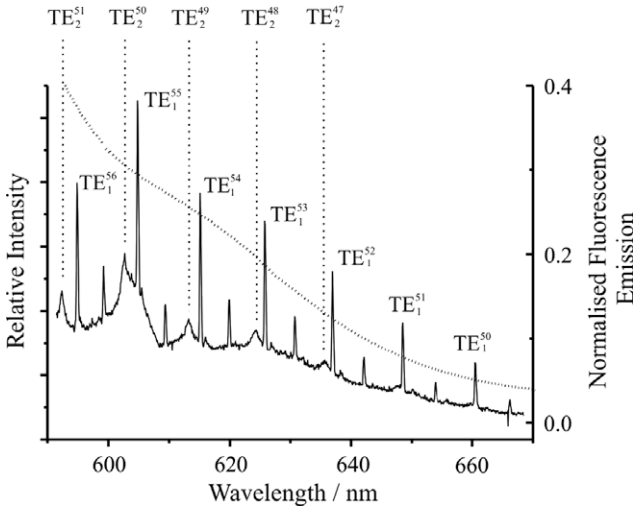

Fig. 11. Cavity-enhanced fluorescence emission spectrum from an aqueous droplet of radius 4.40 μm containing Rhodamine B. A curved dotted line shows the normalised fluorescence emission from a bulk sample of Rhodamine B (data taken from Ref. [104]). The peak centred at ~605 nm arises from Raman scattering by the microscope immersion oil.

with changing laser power is shown in (a). The associated size change is shown in part (b) and a typical spectrum in (c). Such an approach can be used to determine the temperature change of the droplet with a precision of ±0.1 mK [85]. By comparing the derived temperature changes with predictions from Beer–Lambert's law, the absorption coefficient of the droplet solution can be determined. By isolating a second 'control' droplet held at a constant trapping power, the size change of the first droplet can be attributed with confidence to a change in absorption and temperature rather than RH.

The ability to precisely monitor evolving droplet size has provided remarkable insight into the factors determining the droplet vapour pressure [86]. For a droplet growing under conditions of steadily increasing RH, the size is not observed to increase continuously. Rather, the droplet size is observed to undergo periods of smooth growth followed by intervals during which the size appears to remain constant. Following a period of constant size, the droplet is observed to suddenly increase in size before it enters another phase of smooth growth. This behaviour is in contrast to the steady uptake observed in electrostatic-trap measurements and can be attributed to droplet interactions with the optical trap.

During the periods of smooth growth the droplet vapour pressure remains in equilibrium with that of the surroundings *via* uptake of water and hence dilution of the solute. The periods of almost stable size are associated with the droplet approaching a size that is commensurate with a WGM that is resonant with the 532 nm trapping laser. Under these conditions the droplet undergoes resonant heating: the increasing RH of the surroundings is balanced by an increasing droplet vapour pressure arising from an increased temperature as the droplet tunes closer to resonance with the laser, rather than by a compositional change through condensational growth. Once the droplet size exactly matches and then surpasses the resonance condition, the droplet cools instantaneously and the dilution of the solute once again takes over in governing the balancing of the droplet vapour pressure and surrounding RH.

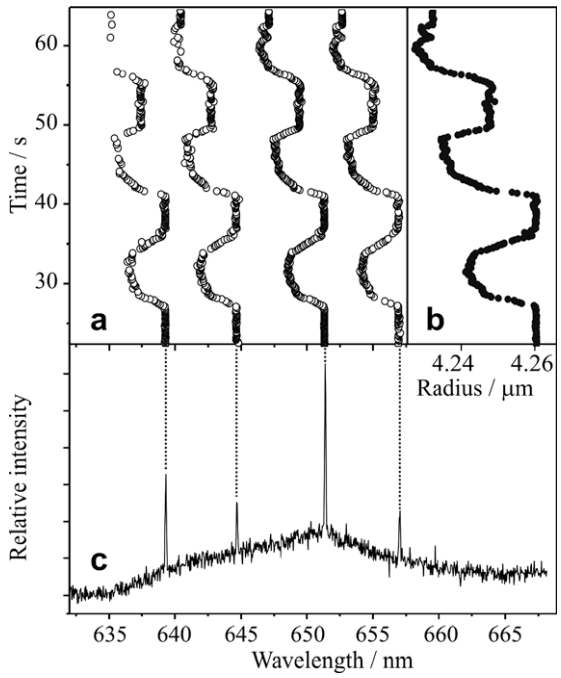

Fig. 12. The effect of changing laser power on droplet size. (a) Resonant modes are seen to move in wavelength synchronously with changes in laser power. (b) The fluctuations in size are of the order of 20 nm in this measurement. (c) The spectrum for the droplet at the beginning of the time sequence in (a).

Even when the resonance condition is perfectly matched by the droplet size, we have shown that the droplet temperature elevation due to resonant heating is an order of magnitude smaller than the level of non-resonant heating observed off-resonance. This suggests that the incident 532 nm light is only weakly coupled into the resonant mode, with a coupling efficiency estimated to be $\sim 1 \times 10^{-3}$ [87]. The periods at which the resonant mode structure appears to remain stable through the establishment of a steady size could provide a mechanism for locking the size of the continuously-tuneable optical cavity formed by the water microdroplet.

4. Environmental control

Controlling and characterising an aerosol particle is not sufficient to explore the factors governing aerosol properties and the dynamics of aerosol transformation. The facile coupling between the gas and condensed phases requires that the gas-phase composition and temperature be robustly controlled and characterised. In this section, we describe briefly the environmental control and monitoring that can be applied.

A first approach for treating the environment surrounding a trapped particle can be described as passive, allowing the conditions in the trapping cell to evolve and avoiding active control. At first glance, this can appear to be fraught with problems: natural variability in the conditions arises from both spatial as well as temporal variability. Common probes for environmental conditions, such as RH, can be slow in time-response, unable to provide the level of accuracy required and unsuited to the dynamic range experienced by the particle. Typical RH probes can have a time-response of ~1 min, an accuracy of ±2%, and may be unable or inaccurate in characterising extreme highs and lows in RH. In addition, probes are necessarily macroscopic, not an ideal match to the microscopic length scales over which aerosol dynamics may be occurring. However, we have introduced the concept of using a control droplet as a highly responsive and accurate microprobe of the local environment of a further droplet of interest. In this way, the RH can be determined with an accuracy of <±0.09%, a time-response of <1 s, and a dynamic range that is exactly matched to the dynamic range required for characterising the second droplet, with measurements possible with the same level of accuracy even up to an RH approaching saturation [52,53]. Although we have so far only demonstrated the use of a microprobe control droplet for determining RH, it is plausible that such a probe droplet could be used to map out the evolution in other environmental conditions such as temperature or the concentration of water soluble components present in the gas phase.

Recently, we have demonstrated that the RH can be actively controlled using an approach that is employed in more conventional experiments, through the mixing of humidified wet and dry nitrogen [88]. This allows the trapped aerosol to be retained within an environment with a RH from <10% to >90%. The RH can be determined using a conventional probe with an accuracy of ±2% and a time-response of ~1 min. Caution must be used when such data is interpreted as the trapped droplet can show immediate equilibration to the environment on sub-second timescales, while the probe data lags behind. Small and rapid fluctuations in particle size due to variations in the local RH of $\ll$2% may not show high correlation with the probe reading due to the mismatch in accuracy and time-response.

The deposition of water soluble or insoluble organics on trapped aerosol can be achieved through gas-phase adsorption, controlled coalescence between aerosol particles generated by nebulisation, or through the controlled flow of sub-micron aerosol generated by homogeneous nucleation following the rapid cooling of a saturated gas. The deposition of oleic acid in aqueous aerosol has been achieved by this latter method. A reservoir of the liquid

is heated to ~100 °C and dry nitrogen is passed above the surface of the liquid. Once the saturated oleic acid gas leaves the confines of the heated reservoir, rapid cooling leads to supersaturation and the homogeneous nucleation of small particles. The flow of small particles can be introduced directly into the immediate vicinity of a trapped droplet. Individual coalescence steps can be monitored by the step-wise growth in the Raman signature of the organic component from the trapped droplet. Recent developments have seen the introduction of a gas flow of a reactive species, ozone, into the vicinity of the trapped droplet at concentrations <500 ppb. Under these conditions, the RH can be maintained at a constant value while an oxidative aging of organic components is monitored.

A particular strength of the optical tweezing strategy for characterising aerosol dynamics is the robustness of the trap governed by the strength of the gradient force which constantly acts to restore the particle to an equilibrium trapping position. A particle can be retained within a variable gas flow, allowing the gas composition to be rapidly changed. Further, the trapped droplet is impervious to collisions with other aerosol droplets that are free-flowing within the gas phase. Thus, coalescence can be used to dope trapped droplets with fluorescing dye, with a hydrophobic/insoluble component that cannot be nebulised within the aqueous phase, or with a droplet containing a chemical reagent that could then initiate a chemical reaction. Finally, the droplet can be retained in the trap even with reduction in pressure: measurements can now be performed on the same aqueous droplet from a pressure of 100 kPa down to 2 kPa, a lower limit that is set by the vapour pressure of water.

5. Frontiers in aerosol optical control and characterisation

We highlighted in Section 1 the potential of applying aerosol techniques to studies of fundamental processes in physical chemistry/chemical physics, using aerosol optical tweezing and Raman spectroscopy as an approach for addressing a broad range of scientific challenges. Expressed in a conventional sense, aerosol properties and processes are often interpreted and predicted from the measurement of bulk properties. However, the elegance of aerosol optical tweezing measurements when coupled with linear and non-linear spectroscopy could allow previously unrealisable detail to be achieved in resolving surface processes, optical properties, intermolecular forces, and heterogeneous chemistry. Such studies could provide and invaluable means for tackling scientific challenges in a broader range of scientific fields than just aerosol science. In this section, we review the potential application of aerosol optical tweezers to a wide range of problems, while also addressing their application to more conventional problems in aerosol science.

5.1. Aerosol sampling

The application of aerosol optical tweezers to date has been limited to the development of aerosol traps, the spectroscopic characterisation of particles, and measurements of the factors governing the equilibrium size of wet aerosol of atmospheric relevance. Frequent and continuous developments in this field, however, have ensured that it is far from reaching maturity. One of the growing challenges is sampling representative aerosols, since both the chemistry and physics of atmospheric aerosols are complex and variable. The established approach is to generate aerosols in the laboratory from stock solutions as simplified proxies for atmospheric aerosols. Such measurements are an invaluable piece of the puzzle, providing thermodynamic and kinetic information for atmospheric models.

Oftentimes, however, models must rely on the extrapolation of data well beyond the range of observation to allow for experimental inflexibilities with respect to, for example, temperature and size. Thus, there is clearly a demand for expansion of laboratory experiments to extend over a greater range in size, RH, pressure and temperature; a move towards a stand-alone instrument that could capture and analyse aerosol particles *in situ* from non-optimised environmental conditions would also be hugely advantageous. Greater control over the gas-phase composition has been discussed earlier in terms of RH control. Reid and co-workers have shown how RH and pressure can be coarsely adjusted in a small volume optical trapping chamber [88]. Integration of temperature control will bring another dimension to the experimental measurements and facilitate studies on the freezing of aqueous droplets, nucleation and phase transitions.

The behaviour of small droplets deviates from their bulk properties as a function of the increasing surface curvature and surface-to-volume ratio associated with decreasing particle radius. Aerosol optical tweezers have proved effective at trapping particles in the size range 1–10 μm in radius. Atmospherically, it is an important goal to push the lower size limit into the accumulation mode (<1 μm). Aerosols in this size range make up the dominant mass fraction of all aerosols in the atmosphere. Very recently, Reid et al. have demonstrated that accumulation mode particles can be trapped in a Bessel beam trap [59]. Although the reasons for the lower size limit of standard tweezers are not well understood, the Bessel beam may present a solution. Optically characterising such small droplets, however, presents a number of new challenges, not least as the particles approach the diffraction limit for visible light.

Bessel traps have a number of additional advantages over optical tweezers. Firstly, the trapping volume within the beam is significantly larger and it is possible to trap particles some distance away from any optical surface, which may affect the gas phase in its immediate vicinity. As such, the Bessel trap has greater potential for forming the basis of an analytical instrument for single particle sampling or *in situ* measurement. Furthermore, one can trap several particles along the propagation length of the Bessel beam and translate particles over a millimetre to centimetre length scale. One can imagine a conveyer belt of sub-micron particles *en-route* to a characterisation region intersecting the trapping beam. The trade off, however, is trap rigidity and optical tweezers are far more robust, displaying a far stronger optical restoring force on the particle motion. Despite this drawback, it should be possible to integrate Bessel beam traps into more complex optical landscapes consisting of many optical tweezers, all under the control of a spatial light modulator.

Departing briefly from radiation pressure traps, manipulation of aerosol particles over macroscopic distances has also been demonstrated by harnessing photophoretic forces. Using two counter-propagating, co-rotating Laguerre–Gaussian laser beams, Desyatnikov and co-workers have been able to transport absorbing carbon particles over distances in excess of 2 m at speeds of up to 1 cm s^{-1} [89,90]. In the case of radiation pressure traps, lasers and particles are chosen such that absorption is minimal, if not negligible. In contrast, photophoretic trapping capitalises on the absorption properties of the particle to create a temperature gradient through it. Molecules of gas colliding with the particle will leave with a greater velocity on the hot side that the cold side, and it is this discrepancy that creates a motive force.

5.2. Aerosol digital microfluidics

The delicate manipulation and exquisite resolution of aerosol optical tools create a powerful platform for study and analysis of fundamental aerosol properties and for performing analytical chemistry or synthetic chemistry on the picolitre scale. Such a small-scale approach bears considerable advantages over macro-

scale alternatives, in particular in terms of time and cost. Microfluidic devices, consisting of micron-sized reaction vessels and capillary tubes etched onto a solid substrate, have been commonplace for a decade or so and are increasing in number and complexity [91]. Applications are abundant and wide-ranging, extending from drug research to point of care medical diagnostics and environmental monitoring. Optical diagnostic techniques have a natural home in these devices where sensitive, non-invasive characterisation is a common prerequisite for efficient functionality. Increasingly, however, optical manipulation methods are also finding applications in microfluidic chips, replacing less versatile mechanical pumps and valves [92]. Despite these gains, the permanent architecture of such devices remains a significant disadvantage for some applications, providing little or no flexibility to accommodate a development in the analytical procedure or assay.

Using optical forces it is becoming possible to replace the entire physical architecture of microfluidic chips and perform micro-assays in picolitre droplets with the additional flexibility of a completely adaptable optical architecture. Chiu and co-workers have demonstrated the distinct advantages that can be realised through the controlled coalescence of aqueous droplets dispersed in oil and trapped within a Laguerre–Gaussian beam [93]. Indeed, by varying the degree of optically-induced heating by variation of laser power, the solute/reactant concentrations within the aqueous phase can be tuned, even allowing access to supersaturated solute states, a concentration range that cannot be explored in typical bulk solution or lab-on-a-chip studies.

We have already seen that, as early examples of the application of holographic aerosol optical tweezers, comparative hygroscopicity measurements on five aerosol droplets held in a carousel array have been performed and controlled and sequential coalescence has been demonstrated [63]. Optical forces have also been used to direct free-flowing aerosol, effectively isolating a single, trapped droplet, and to allow the controlled coalescence of two droplets of differing composition. These procedures meet the criteria of digital microfluidic operations. With the diagnostic tools of Raman, fluorescence and absorption spectroscopies at the immediate disposal of optical tweezing techniques, and the optical landscaping capabilities of spatial light modulation, aerosol HOTs could soon become a powerful technique for microfluidic analysis, particularly in providing a unique platform for the analysis of aerosols. Not only could supersaturated droplets of reactants be prepared by controlling the RH of the environment, but the addition of potential reagents/analytes could be controlled through gas-phase deposition rather than by the requirement to load pre-prepared droplets with appropriate composition. Further, one can imagine a Bessel beam or an alternative droplet-on-demand generator feeding droplets into such an array for analysis, or the *in situ* sampling and analysis of ambient aerosol.

5.3. Aerosol properties and dynamics

We have demonstrated that comparative measurements can be made on multiple particles using aerosol optical tweezers. In particular, we have studied the hygroscopic properties of mixed component aqueous/inorganic/organic aerosol, comparing the evolving wet size of a dicarboxylic acid/sodium chloride or dicarboxylic acid/ammonium sulphate droplet with an aqueous droplet containing the inorganic solute alone [53]. Measurements were performed at RHs close to saturation (>95%), conditions that are challenging to characterise in conventional measurements but are facile when using a second droplet as an RH probe. At such high humidities, the solution thermodynamics can be easily treated as the solutes are at low concentration. However, considering the influence of surface curvature becomes increasingly important on approaching the limit of saturation in RH and this remains true even for the coarse particles that are studied with a gradient force trap. Depressions in size of tens of nanometres are to be expected for particles of a few micrometres in radius when the surface curvature effect is included in the equilibrium size prediction, and the measurement technique provides this required level of sizing accuracy.

At the low RHs that are now accessible in optical tweezing experiments, we are able to study the properties of droplets containing solutes at concentrations higher than saturation. Indeed, given the size range that is accessible and the optical nature of the measurement, these measurements are complementary to the electrostatic single particle measurements that have been routinely used to interrogate supersaturated solute states. Such techniques could allow studies of nucleation and phase change: we have already demonstrated that the timescale of crystallisation, the motion of an inclusion within a host droplet and the homogeneity in refractive index within a trapped particle can be probed [68]. When coupled with the ability to control temperature, the equilibrium state of aerosol could be studied over a wide range of environmental parameters. Further, the dynamics of processes in supersaturated droplets could be investigated.

Much of the discussion has focussed on homogeneous/aqueous aerosol. However, we have already demonstrated that aerosol optical tweezers can be used to interrogate the mixing state and microstructure of hydrophobic and hydrophilic components [70,72,81]. The equilibrium structure of a particle has been shown to be dependent on not only the surfacial and interfacial tensions, but the relative volumes of the hydrophobic and hydrophilic phases. Further, the micro-structure must be considered to be highly dependent on the RH and the volume of water partitioned to the condensed phase. Optical tweezers can provide an ideal approach for characterising the dependence of the micro-structure on water activity, including an assessment of the uniformity of immiscible surface films.

A further avenue that is currently being explored is heterogeneous chemistry and, in particular, the oxidation of aerosol components. To explore atmospheric aerosol aging, it is necessary to expose aerosol to an oxidant concentration over a time window that is comparable to that typical of atmospheric aerosol. Not only can optical tweezers be used to retain a single particle indefinitely, but the evolving hygroscopicity, mixing state and composition can be routinely probed.

The relative importance of thermodynamic factors in controlling particle size and composition, and the kinetic factors that may regulate the rate of approach to the equilibrium state is yet to be fully resolved, particularly for typical atmospheric aerosol containing a high mass fraction of organic components [94]. The fine resolution that can be achieved for recording evolving particle size using optical tweezers could provide a unique approach for resolving the rate of mass accommodation and for interpreting the kinetics of droplet growth or evaporation. In particular, a critical goal is to investigate the influence of surface active organic components on the mass accommodation coefficient of water adsorbing to the surface of a solution droplet. Such measurements could be pursued by comparing the growth or evaporation kinetics of two droplets of different composition in the same environment simultaneously, a kinetic variant on the thermodynamic measurements that have been already demonstrated.

5.4. Aerosols as probes

The opportunity to resolve the mass accommodation of gas-phase water at the surface of a droplet is not only relevant to atmospheric aerosol, but to the mass and heat transfer occurring in aerosol more generally. In addition, it is a prime example of the opportunity offered by aerosol optical tweezers to study a process

of fundamental interest to physical chemists. Further, the fine control that can be achieved on the relative positions of multiple particles held in parallel optical traps could allow the first direct studies of inter-droplet coupling in dense aerosol sprays.

Not only could compositional and kinetic coupling be investigated, but the interaction of aerosol particles is an area that has not been fully explored. The interaction forces experienced by two particles with decreasing interparticle separation could be investigated using techniques analogous to those that have been used in condensed phase optical tweezers. Trapped particles exhibit Brownian diffusion constrained by the restoring optical force. Interparticle interactions can be interrogated by recording the dependence of the trajectories of the trapped particles, either by video microscopy or using a quadrant photodiode [66], on interparticle separation. Not only could this provide invaluable information on the surface forces involved, an important fundamental problem in, for example, tribology, but the dynamics of particle coagulation could be fully explored. Indeed, both surfaces need not be trapped aerosol and one could be a solid flat surface. Under these conditions, the nature of particle–surface interactions could be explored. Recently, McGloin and co-workers have investigated the nature of the viscous damping that must be considered as an aerosol particle is brought close to a flat solid substrate [66].

Takaya and co-workers have developed novel nano-coordinate measuring machines for the determination of the dimensions of microproducts such as microgears and microlenses. Three approaches have been demonstrated, each of which uses an optically-trapped glass microsphere as a probe. Two of the approaches depend on the change in the degree of viscous damping as the probe is brought close to a surface. In the first the boundary of the micro-object is located by detecting a change in the vibrational conditions of the trapped microsphere, and by scanning the probe in three dimensions the shape and size of a micro-object can be determined with an accuracy of around ±30 nm [95]. The second technique involves using a tweezed microsphere which is undergoing circular motion in the plane perpendicular to the trapping laser axis. As the probe approaches a surface the orbit of the sphere becomes elliptical and by analysis of the shape of the orbit the location and normal vector direction of the surface can be determined [96]. In the final approach it was demonstrated that as a fibre-trapped microsphere comes into contact with a surface it is displaced from the central axis of the fibre, giving rise to a change in the amount of light which is reflected back into the trapping fibre and providing a means to locate the surface of a micro-object [97].

Aerosol optical tweezers could provide further insight into the nature of the optical forces that operate between particles. The formation of ordered particle arrays in liquids through the action of optical binding has received considerable interest [98–102]. Each particle must be considered to not only reside in an optical landscape established by the trapping laser beam, but also by the light scattering field established by all other particles in close proximity. The formation of 2d and 3d structures is of particular interest [98,100]. Given the considerably larger refractive index mismatch that accompanies measurements in the gas phase, the nature of the optical forces must be compared with measurements in the condensed phase.

Finally, aerosol droplets could be used as probes of the gas-phase environment. While we have shown that aerosol droplets can be used as a highly responsive and accurate probe of RH, more widespread application to analyse the gas phase is possible. Further, the optical properties of trapped aerosol are yet to be fully exploited. With optical properties typical of high-finesse optical cavities, aerosol droplets could be used to study non-linear optical processes such as four-wave mixing. The quality of high finesse modes could also be used to sense directly the presence of chosen analytes in the surrounding environments.

6. Conclusions

Optical manipulation of aerosol particles has evolved from a novelty to a powerful analytical tool within aerosol science. We have shown that frontier developments in this field are now finding applications in more general areas of chemistry, physics and biology. Indeed, we hope that the potential, as described here, of tweezed liquid aerosols as gas-phase probes, microfluidic reaction vessels and as a platform to confront fundamental, typically bulk phase, chemical problems, will continue to attract more researchers to this growing, interdisciplinary field.

Ackowledgements

The authors gratefully acknowledge support from the EPSRC through the award of a Leadership Fellowship (JPR) and Post-Doctoral Research Fellowships (JBW and KJK).

References

[1] A. Abo Riziq, C. Erlick, E. Dinar, Y. Rudich, Chem. Phys. 7 (2007) 1523.
[2] R. Irshad, R.G. Grainger, D.M. Peters, R.A. McPheat, K.M. Smith, G. Thomas, Atmos. Chem. Phys. 9 (2009) 221.
[3] E.R. Gibson, P.K. Hudson, V.H. Grassian, J. Phys. Chem. A 110 (2006) 11785.
[4] P. Pradeep Kumar, K. Broekhuizen, J.P.D. Abbatt, Chem. Phys. 3 (2003) 509.
[5] M. Mochida, Y. Katrib, J.T. Jayne, D.R. Worsnop, S.T. Martin, Atmos. Chem. Phys. 6 (2006) 4851.
[6] P.K. Mogili, P.D. Kleiber, M.A. Young, V.H. Grassian, J. Phys. Chem. A 110 (2006) 13799.
[7] R.M. Garland, M.E. Wise, M.R. Beaver, H.L. DeWitt, A.C. Aiken, J.L. Jimenez, M.A. Tolbert, Atmos. Chem. Phys. 5 (2005) 1951.
[8] P.T. Griffiths, C.L. Badger, R.A. Cox, M. Folkers, H.H. Henk, T.F. Mentel, J. Phys. Chem. A 113 (2009) 5082.
[9] G. Biskos, A. Malinowski, L.M. Russell, P.R. Buseck, S.T. Martin, Aerosol Sci. Technol. 40 (2006) 97.
[10] B. Svenningsson et al., Atmos. Chem. Phys. 6 (2006) 1937.
[11] S. Takahama, R.K. Pathak, S.N. Pandis, Environ. Sci. Technol. 41 (2007) 2289.
[12] J.C. Reynolds et al., Environ. Sci. Technol. 40 (2006) 6674.
[13] M.A. Fernandez, R.G. Hynes, R.A. Cox, J. Phys. Chem. A 109 (2005) 9986.
[14] H.A. Al-Hosney, S. Carlos-Cuellar, J. Baltrusaitis, V.H. Grassian, Phys. Chem. Chem. Phys. 7 (2005) 3587.
[15] C.E. Lund Myhre, C.J. Nielsen, Chem. Phys. 4 (2004) 1759.
[16] S. Seisel, A. Pashkova, Y. Lian, R. Zellner, Faraday Discuss. 130 (2005) 437.
[17] A.K. Lee, C.K. Chan, Atmos. Environ. 41 (2007) 4611.
[18] A.K.Y. Lee, C.K. Chan, J. Phys. Chem. A 111 (2007) 6285.
[19] A.K.Y. Lee, T.Y. Ling, C.K. Chan, Faraday Discuss. 137 (2008) 245.
[20] M.N. Chan, A.K.Y. Lee, C.K. Chan, Environ. Sci. Technol. 40 (2006) 6983.
[21] L. Treuel, S. Schulze, T. Leisner, R. Zellner, Faraday Discuss. 137 (2008) 265.
[22] C. Mund, R. Zellner, J. Mol. Struct. 661–662 (2003) 491.
[23] C.A. Colberg, U.K. Krieger, T. Peter, J. Phys. Chem. A 108 (2004) 2700.
[24] P. Stockel, I.M. Weidinger, H. Baumgartel, T. Leisner, J. Phys. Chem. A 109 (2005) 2540.
[25] C. Marcolli, U.K. Krieger, J. Phys. Chem. A 110 (2006) 1881.
[26] A.K. Ray, A. Souyri, E.J. Davis, T.M. Allen, Appl. Opt. 30 (1991) 3974.
[27] U.K. Krieger, A.A. Zardini, Faraday Discuss. 137 (2008) 377.
[28] M.L. Shulman, R.J. Charlson, E. James, J. Aerosol Sci. 28 (1997) 737.
[29] D.C. Taflin, S.H. Zhang, E. James Davis, AIChE J. 34 (1988) 1310.
[30] E.J. Davis, Aerosol Sci. Technol. 26 (1997) 212.
[31] J.P. Reid, J. Quant. Spectrosc. Radiat. Transfer 110 (2009) 1293.
[32] G. Schweiger, J. Aerosol Sci. 21 (1990) 483.
[33] P.N. Lebedev, Ann. der Physik 6 (1901) 433.
[34] A. Ashkin, Phys. Rev. Lett. 24 (1970) 156.
[35] K. Dholakia, P. Reece, M. Gu, Chem. Soc. Rev. 37 (2008) 42.
[36] J.E. Molloy, M.J. Padgett, Contemporary Phys. 43 (2002) 241.
[37] A. Ashkin, J.M. Dziedzic, Appl. Phys. Lett. 19 (1971) 283.
[38] A. Ashkin, J.M. Dziedzic, Science 187 (1975) 1073.
[39] A. Ashkin, J.M. Dziedzic, Appl. Opt. 19 (1980) 660.
[40] A. Ashkin, J.M. Dziedzic, Appl. Phys. Lett. 24 (1974) 586.
[41] R. Pfeifer, T. Nieminen, N. Heckenberg, H. Rubinsztein-Dunlop, Rev. Mod. Phys. 79 (2007) 1197.
[42] H. Minkowski, Nachr. Ges. Wiss.Gött. (1908) 53.
[43] M. Abraham, Rendiconti del Circolo Matematico di Palermo (1884–1940) 28 (1909) 1.
[44] G. Roosen, C. Imbert, Phys. Lett. A 59 (1976) 6.
[45] M. Guillon, O. Moine, B. Stout, Phys. Rev. Lett. (2006) 96.
[46] D. Rudd, C. Lopez-Mariscal, M. Summers, A. Shahvisi, J.C. Gutiérrez-Vega, D. McGloin, Opt. Exp. 16 (2008) 14550.
[47] A. Ashkin, J.M. Dziedzic, J.E. Bjorkholm, S. Chu, Opt. Lett. 11 (1986) 288.
[48] R. Omori, T. Kobayashi, A. Suzuki, Opt. Lett. 22 (1997) 816.

[49] N. Magome, M.I. Kohira, E. Hayata, S. Mukai, K. Yoshikawa, J. Phys. Chem. B 107 (2003) 3988.
[50] E.F. Fallman, O. Axner, Appl. Opt. 36 (1997) 2107.
[51] L. Mitchem, R.J. Hopkins, J. Buajarern, A.D. Ward, J.P. Reid, Chem. Phys. Lett. 432 (2006) 362.
[52] J.R. Butler, L. Mitchem, K.L. Hanford, L. Treuel, J.P. Reid, Faraday Discuss. 137 (2008) 351.
[53] Kate L. Hanford, Laura Mitchem, Jonathan P. Reid, Simon L. Clegg, David O. Topping, Gordon B. McFiggans, J. Phys. Chem. A 112 (2008) 9413.
[54] J. Buajarern, L. Mitchem, A.D. Ward, N.H. Nahler, D. McGloin, J.P. Reid, J. Chem. Phys. 125 (2006) 114506.
[55] S. Sato, M. Ishigure, H. Inaba, Electron. Lett. 27 (1991) 1831.
[56] N.B. Simpson, K. Dholakia, L. Allen, M.J. Padgett, Opt. Lett. 22 (1997) 52.
[57] D. McGloin, D.R. Burnham, M.D. Summers, D. Rudd, N. Dewar, S. Anand, Faraday Discuss. 137 (2008) 335.
[58] J. Durnin, J.J. Miceli, J.H. Eberly, Phys. Rev. Lett. 58 (1987) 1499.
[59] H. Meresman, J.B. Wills, M. Summers, D. Mcgloin, J.P. Reid, Phys. Chem. Chem. Phys., in press.
[60] R.L. Eriksen, V.R. Daria, J. Gluckstad, Opt. Exp. 10 (2002) 597.
[61] J.E. Curtis, B.A. Koss, D.G. Grier, Opt. Commun. 207 (2002) 169.
[62] D.R. Burnham, D. McGloin, Opt. Exp. 14 (2006) 4175.
[63] Jason R. Butler, Jon B. Wills, Laura Mitchem, Dan Burnham, David McGloin, Jonathan P. Reid, Lab on a Chip 9 (2009) 521.
[64] J.B. Wills, J. Butler, J. Palmer, J. Reid, Phys. Chem. Chem. Phys. (2009), doi:10.1039/b908270k.
[65] J.P. Reid, in: T. Cosgrove (Ed.), Colloid Science: Theory, Methods and Application, Blackwell Publishing, Oxford, 2005, p. 180.
[66] D. Burnham, D. McGloin, New J. Phys. (2009) 11.
[67] K.J. Knox, J.P. Reid, K.L. Hanford, A.J. Hudson, L. Mitchem, J. Opt. A: Pure Appl. Opt. 9 (2007) S180.
[68] A.M.C. Laurain, J.P. Reid, J. Phys. Chem. A 113 (2009) 7039.
[69] J. Buajarern, L. Mitchem, J. Reid, J. Phys. Chem. A 111 (2007) 13038.
[70] J. Buajarern, L. Mitchem, J. Reid, J. Phys. Chem. A 111 (2007) 9054.
[71] S. Torza, S.G. Mason, J. Colloid Interf. Sci. 33 (1970) 67.
[72] L. Mitchem, J. Buajarern, A. Ward, J. Reid, J. Phys. Chem. B 110 (2006) 13700.
[73] L. Mitchem, J.P. Reid, Chem. Soc. Rev. 37 (2008) 756.
[74] L. Mitchem, J. Buajarern, R. Hopkins, A. Ward, R. Gilham, R. Johnston, J. Reid, J. Phys. Chem. A 110 (2006) 8116.
[75] H. Meresman, A. Hudson, J.P. Reid, in preparation.
[76] M. King, K. Thompson, A. Ward, J. Am. Chem. Soc. 126 (2004) 16710.
[77] M. King, K. Thompson, A. Ward, C. Pfrang, B. Hughes, Faraday Discuss. 137 (2008) 173.
[78] H.B. Lin, J.D. Eversole, A.J. Campillo, Rev. Sci. Instrum. 61 (1990) 1018.
[79] R. Symes, R.M. Sayer, J.P. Reid, Phys. Chem. Chem. Phys. 6 (2004) 474.
[80] U. Poschl, Angew. Chem., Int. Ed. 44 (2005) 7520.
[81] J. Buajarern, L. Mitchem, J. Reid, J. Phys. Chem. A 111 (2007) 11852.
[82] J.D. Eversole, H.B. Lin, C.D. Merritt, A.J. Campillo, Appl. Spectrosc. 48 (1994) 373.
[83] A.D. Ward, M. Zhang, O. Hunt, Opt. Exp. 16 (2008) 16390.
[84] J. Buajarern, Ph.D., University of Bristol, Bristol, UK, 2007.
[85] K. Knox, J. Reid, J. Phys. Chem. A 112 (2008) 10439.
[86] R.E.H. Miles, M. Guillon, L. Mitchem, D. Mcgloin, J.P. Reid, PCCP 11 (2009) 7312.
[87] M. Guillon, R.E.H. Miles, J.P. Reid, D. McGloin, New J. Phys., in press.
[88] N. Kwamena, G. Hargreaves, J.P. Reid, in preparation.
[89] V.G. Shvedov, A.S. Desyatnikov, A.V. Rode, W. Krolikowski, Y.S. Kivshar, Opt. Exp. 17 (2009) 5743.
[90] A.S. Desyatnikov, V.G. Shvedov, A.V. Rode, W. Krolikowski, Y.S. Kivshar, Opt. Exp. 17 (2009) 8201.
[91] S. Teh, R. Lin, L. Hung, A.P. Lee, Lab on a Chip 8 (2008) 198.
[92] H. Mushfique, J. Leach, R. Di Leonardo, M.J. Padgett, J.M. Cooper, Proc. Inst. Mech. Eng. Part C: J. Mech. Eng. Sci. 222 (2008) 829.
[93] R. Lorenz, J. Edgar, G. Jeffries, Y. Zhao, D. McGloin, D. Chiu, Anal. Chem. 79 (2007) 224.
[94] M.N. Chan, C.K. Chan, Atmos. Chem. Phys. 5 (2005) 2703.
[95] M. Michihata, Y. Takaya, T. Hayashi, CIRP Ann. – Manufact. Technol. 57 (2008) 493.
[96] M. Michihata, Y. Nagasaka, T. Hayashi, Y. Takaya, Appl. Opt. 48 (2009) 198.
[97] S.I. Eom, Y. Takaya, T. Hayashi, Precis. Eng. 33 (2009) 235.
[98] M.M. Burns, J. Fournier, J.A. Golovchenko, Phys. Rev. Lett. 63 (1989) 1233.
[99] M.M. Burns, J. Fournier, J.A. Golovchenko, Science 249 (1990) 749.
[100] S.A. Tatarkova, A.E. Carruthers, K. Dholakia, Phys. Rev. Lett. 89 (2002) 283901.
[101] W. Singer, M. Frick, S. Bernet, M. Ritsch-Marte, J. Opt. Soc. Am. B 20 (2003) 1568.
[102] D. McGloin, A.E. Carruthers, K. Dholakia, E.M. Wright, Phys. Rev. E 69 (2004) 021403.
[103] K.J. Knox, Ph.D., University of Bristol, Bristol, UK, 2009.
[104] H. Du, R. Fuh, J. Li, L. Corkan, J. Lindsey, Photochem. Photobiol. 68 (1998) 141.

Jon Wills received his B.Sc., in Chemistry and Astronomy at the University of Sheffield in 1999 and his Ph.D. from the University of Bristol in 2002. His thesis focussed on the development and application of cavity ring down spectroscopy. After a year's postdoctoral study at Université Lyon 1 in France, he spent three years in academic publishing and semi-professional sport before returning to Bristol in 2006 to take up a teaching fellowship for one year. This was followed by the move to his current postdoctoral research position studying the thermodynamic and kinetic properties of aerosol droplets using optical tweezers.

Kerry Knox graduated in Natural Sciences from the University of Cambridge (Emmanuel College) in 2004. Following a PGCE at the University of Oxford she carried out doctoral studies at the University of Bristol, receiving her Ph.D. in 2009. She was a Japan Society for the Promotion of Science research fellow at the University of Hokkaido in 2007. Her doctoral thesis concerned optically-induced processes in optically-tweezed aerosol droplets, an area she is continuing to pursue as a postdoctoral researcher at the University of Bristol.

Jonathan Reid studied for his undergraduate and postgraduate degrees from the University of Oxford (M.A., DPhil) before moving to a post-doctoral fellowship at JILA, University of Colorado, USA. In 2000 he took up a lectureship at the University of Birmingham before moving to the University of Bristol in 2004. He is a Professor in Physical Chemistry and an EPSRC Leadership Fellow. He was awarded the 2001 Harrison Memorial Prize and the 2004 Marlow Medal by the Royal Society of Chemistry.